Light-Induced Conformational Changes of Cyanobacterial Phytochrome Cph1 Probed by Limited Proteolysis and Autophosphorylation†

Berta Esteban,‡ Montserrat Carrascal,§ Joaquin Abian,§ and Tilman Lamparter*,‡

Pflanzenphysiologie, Freie Universität Berlin, Königin Luise Strasse 12-16, D-14195 Berlin, Germany, and Structural and Biological Mass Spectrometry Unit, IIBB-CSIC, IDIBAPS, Rosellon 161, 7 Planta E-08036 Barcelona, Spain

Received July 22, 2004; Revised Manuscript Received October 14, 2004

ABSTRACT: Photoreceptor chromoproteins undergo light-induced conformational changes that result in a modulation of protein interaction and enzymatic activity. Bacterial phytochromes such as Cph1 from the cyanobacterium *Synechocystis* PCC 6803 are light-regulated histidine kinases in which the light signal is transferred from the N-terminal chromophore module to the C-terminal kinase module. In this study, purified recombinant Cph1 was subjected to limited proteolysis using trypsin and endoproteinase Glu-C (V8). Cleavage sites of chromopeptide fragments were determined by MALDI-TOF and micro-HPLC on-line with tandem mass spectrometry in an ion trap mass spectrometer. Trypsin produced three major chromopeptides, termed F1 (S56 to R520), F2 (T64 to R472), and F3 (L81 to R472). F1 was produced only in the far-red absorbing form Pfr within 15 min and remained stable up to >1 h; F2 and F3 were obtained in the red-light absorbing form Pr within ca. 5−10 min. When F1 was photoconverted to Pr in the presence of trypsin, this fragment degraded to F2 and F3 within 1−2 min. On size exclusion chromatography, F1 eluted as a dimer in the Pfr and as a monomer in the Pr form, whereas F2 and F3 behaved always as monomers, irrespective of the light conditions. These and other results are discussed in the context of light-dependent subunit interactions, in which amino acids 473−520 within the PHY domain are required for chromophore−module subunit interaction within the homodimer. V8 proteolysis yielded five major chromopeptides, F4 (T17 to N449), F5 (T17 to E335), F6 (T17 to E323), F7 (unknown sequence), and F8 (tentatively L121 to E323). F6 and F8 were formed in the Pr form, whereas F4, F5, and F7 were preferentially formed in the Pfr form. Three amino acids next to specific cleavage sites, R520, R472, and E323, were altered by site-directed mutagenesis. The mutants were analyzed by UV−vis spectroscopy, size exclusion chromatography, and autophosphorylation. Histidine kinase activity was low in R472A, R520P, and R520A; in all mutants, the ratio of phosphorylation intensity between Pr and Pfr was reduced. Thus, light regulation of autophosphorylation is negatively affected in all mutants. In R472P, E323P, and E323D, the phosphorylation intensity of the Pfr form exceeded that of the wild-type control. This result shows that the histidine kinase activity of Cph1 is actively inhibited by photoconversion into Pfr.

Phytochromes are widely distributed biliprotein photoreceptors that are most sensitive in the red or far-red region of the visible spectrum (*1*). The photocycle of typical phytochromes has two thermostable, spectrally different forms that are interconverted by light (*2*). Phytochromes are synthesized in the red-absorbing form, Pr, in a process during which the chromophore becomes autocatalytically attached to a conserved cysteine residue. Photoconversion into Pfr, the far-red absorbing form, is initiated by a rapid isomerization around the C15═C16 double bond of the chromophore (*3*−*5*). Thereafter, thermal relaxations into Pfr are observed in the microsecond and millisecond time range (*6*). Typical phytochrome proteins consist of an N-terminal chromophore module and a C-terminal regulatory module. Within the chromophore module, computer algorithms identify two to three different subdomains. In some bacterial phytochromes, such as Cph1 from the cyanobacterium *Synechocystis* PCC 6803, a PAS domain is found close to the N-terminus of the protein (see Figure 1C for the domain structure of Cph1). In biliverdin-binding phytochromes of proteobacteria, the homologous region bears the chromophore-binding cysteine residue (*7*). The GAF domain is the region of the highest homology among phytochromes. The chromophore-binding cysteine of cyanobacterial and plant phytochromes, which incorporate phycocyanobilin or phytochromobilin, lies within this domain. It has been shown for recombinant fragments of Cph2, a nontypical phytochrome from *Synechocystis*, that the GAF domain is sufficient for the chromophore ligation reaction (*8*).

The C-terminal subdomain of the chromophore module is a so-called PHY domain, which is probably important for spectral integrity. Whereas the entire chromophore module is spectrally identical with the full-length protein (*6*, *9*, *10*), truncated proteins which lack part of the PHY domain are

† This work was supported by the Deutsche Forschungsgemeinschaft, Sonderforschungsbereich 498, Teilprojekt B2.

* Corresponding author. Tel: +49 (0)30 838 54918. Fax: +49 (0)-30 838 84357. E-mail: lamparte@zedat.fu-berlin.de.

‡ Freie Universität Berlin.

§ IIBB-CSIC, IDIBAPS.

10.1021/bi0484365 CCC: $30.25
Published on Web 12/16/2004

characterized by their drastically reduced Pfr absorbance (*9*, *11*, *12*). In phytochromes purified from plants, protein conformational differences between Pr and Pfr have been observed by several techniques including limited proteolysis, cysteine labeling, circular dichroism, and chromatography (*13*−*20*). Conformational changes trigger spectral absorbance changes and phytochrome-initiated signal transduction, but details about the underlying molecular mechanisms are as yet unknown.

Plant phytochromes have a molecular mass of about 124 kDa. The C-terminus is homologous to histidine kinases, but the substrate histidine is often lacking, and histidine kinase activity has not been detected in plant phytochromes. It has been shown that plant phytochromes act as light-regulated serine/threonine kinases (*21*). Prokaryotic phytochromes differ from their plant homologues in several aspects. Typical bacterial phytochromes have a size of about 85 kDa and act as light-regulated histidine kinases. In general, histidine kinase activity is strong in the Pr and weak in the Pfr form (*10*, *22*, *23*). The histidine kinase subunit trans-phosphorylates a response regulator protein in a light-dependent manner (*10*, *22*, *24*, *25*); further steps in the signal transduction cascade are as yet unknown.

The phytochrome Cph1 from the cyanobacterium *Synechocystis* PCC 6803 has been analyzed by a number of biochemical and biophysical methods. Cph1 assembles with phycocyanobilin (PCB),[1] the natural chromophore (*26*), phytochromobilin, and phycoerythrobilin (*10*, *24*, *27*, *28*). Three steps can be spectrally distinguished in the assembly process of Cph1 with PCB: a rapid interaction of the chromophore with the protein, followed by protonation of the chromophore and chromophore stretching, characterized by a red shift of the absorption maximum, and the formation of the covalent bond with C259, which is characterized by a blue shift (*29*). Size exclusion chromatography (*24*) and fluorescence resonance energy transfer (*30*) imply that holo-Cph1 forms homodimers, as other histidine kinases and plant phytochromes, although monomeric Cph1 can be purified under particular conditions (*24*, *31*). Resonance Raman spectroscopy and FTIR measurements showed that the chromophore is folded in a similar way as in plant phytochromes (*32*, *33*). The photocycle of Cph1 is also comparable with plant phytochromes, although a strong deuterium effect for the turnover of an early intermediate has been found, which is not observed with plant phytochromes (*32*). Protonation and deprotonation events during the photocycle have been measured kinetically using fluorescent proton sensors (*6*). Direct indications for light-induced conformational changes of Cph1 have been found by size exclusion chromatography (*24*). In the present study, we analyzed conformational differences between Pr and Pfr by limited proteolysis to gain a deeper insight into the light modulation of histidine kinase activity of this photoreceptor. In our experiments, we found strong differences between the Pr and the Pfr form of Cph1, in contrast to another study, which was performed with a different expression construct (*31*). To determine the position of conformation-specific cleavage sites and to define functions of protein domains, we determined the peptide sequences of prominent chromopeptide fragments by mass spectrometry. The amino acids of three different conformation-specific cleavage sites were altered by site-directed mutagenesis. The mutants were used to test for signal transmission from the chromophore module to the histidine kinase.

[1] Abbreviations: MALDI-TOFMS, matrix-assisted laser desorption−ionization time-of-flight mass spectrometry; nESI-ITMS, nanoelectrospray ion trap mass spectrometry; PAGE, polyacrylamide gel electrophoresis; PCB, phycocyanobilin; V8, endoproteinase Glu-C.

EXPERIMENTAL PROCEDURES

Chromophore and Protein Purification. Phycocyanobilin (PCB) was extracted from *Spirulina geitlerie* by boiling methanolysis and purified by HPLC. The Cph1 protein with a C-terminal polyhistidine is encoded by the pQE12 (Qiagen, Hilden, Germany) derived vector pF10.his (*28*). The protein was purified by affinity chromatography and finally suspended in 50 mM Tris-HCl and 5 mM EDTA, pH 7.8. Details of the purification procedures are given in earlier publications (*24*, *28*). For preparative native electrophoresis, affinity-purifed Cph1 was subjected to a "Prep-Cell" (Bio-Rad) apparatus as described earlier (*24*).

Proteolysis. Before the addition of protease, purified holo-Cph1 (1.5 mg/mL) was irradiated with red (654 nm, 32 μmol m^{-2} s^{-1}) or far-red light (730 nm, 68 μmol m^{-2} s^{-1}) for 5 min to obtain high Pfr and Pr levels, respectively. After the irradiation, Cph1 samples were handled under green safelight or kept in darkness at 18 °C. Trypsin (TPCK-treated; Sigma, Hilden, Germany) or endoproteinase Glu-C (V8, type XVII-B; Sigma) was added to a final concentration of 5 μg/mL. Proteolysis was stopped by the addition of SDS sample buffer (final SDS concentration 2%). Before size exclusion chromatography of trypsin-digested Cph1, proteolysis was stopped by the addition of soybean trypsin inhibitor (Sigma) at a final concentration of 50 μg/mL.

Analytical Gel Electrophoresis. Discontinuous gel electrophoresis (SDS−PAGE) was performed with the Protean I (length of separating gel 5 cm, gel thickness 1 mm) or with the Protean II system (length of separating gel 16 cm, gel thickness 1.5 mm) of Bio-Rad. The gels were prepared according to Laemmli (*34*) with 13% acrylamide/0.3% bisacrylamide in the separating gel and 4% acrylamide/0.1% bisacrylamide in stacking gels. The 3× sample buffer contained 0.5 M Tris-HCl, pH 6.8, 30% glycerol (v/v), 6% SDS (w/v), 0.3 M DTT, and 0.01% (w/v) bromphenol blue. Alternatively, peptides were separated on 12% NuPage gels (Invitrogen) according to the instructions of the manufacturer. Chromopeptides were detected by Zn^{2+} fluorescence (*24*, *35*); thereafter, the peptides were stained with Coomassie.

HPLC and Mass Spectrometry. For sequence determination, peptide mixtures were first separated on SDS−PAGE. The gels were stained with Coomassie, the areas around protein bands were cut out, and the slices were subjected to in-gel trypsin digest as described (*36*). From a 20 min trypsin digest, the F1 (52 kDa) fragment of a red-treated sample and the F2 (49 kDa) and F3 (43 kDa) fragments of a far-red-treated sample were chosen. From a 48 h V8 digest, we chose the F4 (47 kDa), F5 (35 kDa), and F7 (26 kDa) fragments of the red-treated sample and the F6 (34 kDa) and F8 (24 kDa) fragments of the far-red-treated sample. Controls were always made with the full-length Cph1 protein. The fragments were analyzed by MALDI-TOF and with a micro HPLC which was coupled on-line with a tandem mass

spectrometer in an ion trap (*36*). In this way, most fragments that constituted to the peptides were identified. In the case of V8 digested peptides, the start and end fragments were independently identified because the V8 cleavage specificity differs from trypsin.

Mutagenesis. Six mutants with single amino acid exchanges, E323D, E323P, R472A, R472P, R520A, and R520P, were generated by PCR amplification of the expression vector pF10.his with the error checking polymerase TaKaRa Ex (TaKaRa, Shuzo, Japan). The following primers were used: b34, **GAT**ACCTTCGATTACCGGGTGC; b35, CGTATCTTCCTGGGCGGA; b36, **CCA**ACCTTCGATTACCGGGTGC; b42, **GCC**CAATCCTTTGACCTCTGG; b43,GGGATGGAGCTCGATTTTACC; b44, **CCC**CAATCCTTTGACCTCTGG; b45, **GCC**AACTTGGAACGCTCCAACG; b46, GGCTAACTGGGCCAATTCTTC; b47, **CCC**AACTTGGAACGCTCCAACG (mutant codons are given in bold letters). Primer combinations were as follows: E323D, b34/b35; E232P, b36/b35; R472A, b42/b43; R472A, b44/b43; R520A, b45/b46; R520P, b47/b46. The PCRs were carried out with 5 cycles of 94 °C, 1 min; 58 °C, 1 min; 72 °C, 5 min and with 25 cycles of 94 °C, 1 min; 60 or 62 °C, 1 min; 72 °C, 5 min. The 4.7 kbp PCR products were processed with Vent DNA polymerase to remove A overhangs, circularized with T4 DNA ligase (New England Biolabs, Beverly, MA), and transformed into *Escherichia coli*. Correct cloning was confirmed by DNA sequencing.

Expression vectors for deletion proteins were constructed as follows: primers f23 (GGAATTCATTAAAGAGGAGAAATTAACTATGGCCACCACCGTACAACTCG) and b86 (GGGAGATCTTTCCTGGGCGGAAATGTTG) were used to PCR amplify the coding region for amino acids M1 to E323 of Cph1. The construct was cloned via *Eco*RI/*Bgl*II restriction sites into the pQE12 expression vector. Primers b85 (GAATTCATTAAAGAGGAGAAATTAACTATGGAAACCCTCGCCATCCAC) and b86 (see above) were used to PCR amplify the region coding for amino acids T17 to E323 of Cph1 and cloned into pQE12 by the same strategy. The expression clone for amino acids 121−323 was PCR amplified from the T17_E323 expression clone using the primers b98 (CTAGAGCCAGCCTACACT) and b100 (CATAGTTAATTTCTCCTCTTTAATG). The PCR product was blunted and circularized as above. All expressed proteins contain a C-terminal polyhistidine tag for Ni^{2+} affinity purification. Protein expression and Ni^{2+} affinity purification were performed as with the wild-type protein.

Phosphorylation. Autophosphorylation of Cph1 and mutants was performed as described (*24*). Before incubation with [γ-^{32}P]ATP, PCB-Cph1 was irradiated with saturating far-red or red light and incubated in darkness at 20 °C. A fluorescent image analyzer FLA 2000 (Fuji) was used to quantify the signal intensity with an integrated analysis software.

Analytical Size Exclusion Chromatography. Size exclusion chromatography was carried out on a Superdex 200 HR 10/30 (Amersham/Pharmacia, Freiburg, Germany) column run at 500 μL/min with 50 mM Tris-HCl (pH 7.8), 150 mM NaCl, and 5 mM EDTA using a 200 μL sample loop. The system was calibrated with marker proteins cytochrome *c* (12.4 kDa), carbonic anhydrase (29 kDa), bovine serum albumin (66 kDa), alcohol dehydrogenase (150 kDa), β-amylase (299 kDa), and apoferritin (443 kDa) (Sigma). Chromopeptides were monitored at 365 nm and marker proteins and full-length Cph1 and mutants at 280 nm.

RESULTS

Trypsin Digestion, SDS−PAGE, and UV−Vis Spectroscopy. Holo-Cph1 was irradiated with either far-red or red light to adjust a photoequilibrium of about 95% Pr or 70% Pfr, respectively (*28*, *37*) and subjected to proteolysis with trypsin for varying incubation times. After proteolysis, the peptides were separated by SDS−PAGE. Chromophore-bearing peptides (chromopeptides) were detected by Zn^{2+} fluorescence; the same gels were then stained by Coomassie to visualize also chromophore-free peptides (Figure 1A). After a 1 min trypsin treatment, chromopeptides of 49 and 52 kDa were formed; a 85 kDa chromopeptide, probably the undigested full-length protein, was also present. Smaller chromophore-free fragments of 43, 31, and 22 kDa were also formed. The patterns of the far-red- and red-treated samples were similar after a 1 min digestion, but the band intensity of the 52 kDa fragment was slightly weaker and the band intensity of the 49 kDa fragment was slightly stronger in the far-red irradiated sample. During prolonged protease incubation, the difference between both samples became stronger. The 85 kDa chromopeptide was lost after incubation times of 15 min or longer, but three prominent chromopeptides of 43, 49, and 52 kDa were present in both samples up to an incubation time of 1 h. These fragments are denominated F1 (52 kDa), F2 (49 kDa), and F3 (43 kDa). Since F1 appeared faster after red irradiation, the corresponding cleavage sites were specifically exposed in the Pfr form; F2 and F3 were formed faster in the far-red-treated sample, and these cleavage sites must be specifically exposed in the Pr form. It should be noted that saturating red light produces only 70% Pfr. Thus, fragments F2 and F3 of the red-treated sample are probably formed from residual Pr (or from Pr/Pfr heterodimers; see below). After trypsin incubation of 8 h and longer, the F1, F2, and F3 fragments were also digested. Two chromopeptides of 5 and 3 kDa, which were present after both light pretreatments at equal band intensity, appeared. In the time range of 5−15 min, a 3 kDa chromophore-free fragment appeared which was strong after far-red but rather weak after red preirradiation. Most likely, this fragment corresponds to a peptide which is cleaved from the F1 fragment to produce F2. The intensity of other chromophore-free bands did not significantly differ between both light treatments.

We also followed proteolysis by UV−vis spectroscopy (Figure 1B). During digestion, the absorption maximum of the Pr and the Pfr form shifted to shorter wavelengths, and the absorption of both forms was reduced. The Pfr absorption was faster reduced than the Pr absorption, although Cph1 is faster degraded in its Pr form (after far-red irradiation; see Figure 1A). A rather weak Pfr absorbance has been reported for fragments from the N-terminus of plant phytochromes (*9*, *11*). The spectra obtained after 24 h trypsin digestions resembled spectra of the free chromophore. Small spectral differences were observed between both light pretreatments (Figure 1B), which reflect the different isomerization states of the free chromophores. This difference shows that the chromophore is kept in its isomeric state throughout the entire trypsin treatment.

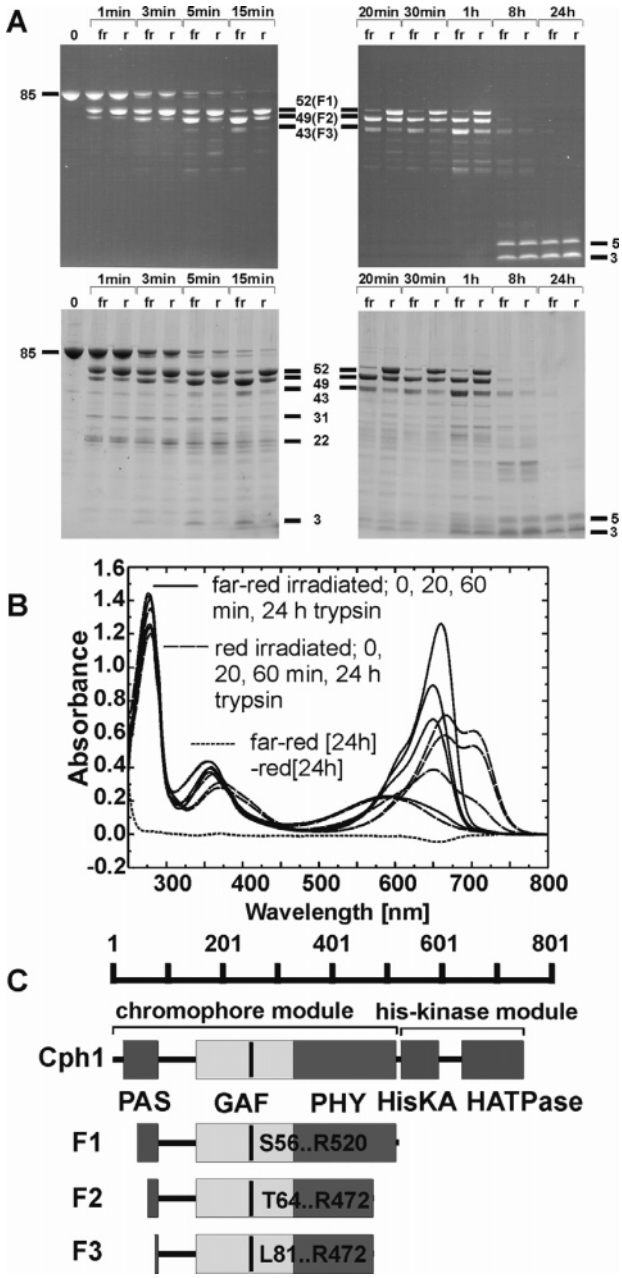

FIGURE 1: Trypsin digestion of Cph1. (A) SDS−PAGE. Cph1 was irradiated with saturating far-red (fr) or red (r) as indicated and treated for 1 min to 24 h with trypsin. 0 = undigested Cph1 control. Above: Zn^{2+}-induced fluorescence. Below: Coomassie stain. The apparent molecular size (kDa) of particular fragments is indicated on the left and right side of the panels. Prominent chromopeptide bands are denominated F1, F2, and F3. (B) UV−vis spectra of Cph1 during trypsin proteolysis after far-red (straight lines) and red irradiation (dashed lines); difference spectrum between the far-red- and red-treated sample after 24 h of trypsin (dotted line). The absorption in the red wavelength region decreases over time. (C) Domain structure of Cph1 and the proteolytic fragments F1−F3 (see also Table 1). The position of the chromophore-binding cysteine is indicated by a black line.

Mass Spectrometry of Trypsin Chromopeptides. The sequences of fragments F1, F2, and F3 were determined by mass spectrometry. From a 15 min trypsin digest, the F1 (52 kDa) fragment of a red-treated sample and the F2 (49 kDa) and F3 (43 kDa) fragments of a far-red-treated sample were chosen. After separation on SDS gels, the excised peptides were completely digested with trypsin and subjected to HPLC chromatography followed by ion trap mass spectrometry (LC-ITMS). Most subfragments that constitute to the entire peptides were detected in the mass spectrometer. A control was also performed with full-length Cph1. In the region next to the N- and C-terminal ends of F1, F2, and F3, all predicted subfragments were detected. Therefore, the borders of the chromopeptides could unambiguously be determined. Results of the mass spectrometry measurements are summarized in Figure 1C and Table 1. The F1 fragment ranges from S56 to R520. The latter amino acid is located in the hinge region between the chromophore module and the C-terminal histidine kinase domain; S56 lies within the PAS domain in the N-terminus of Cph1. F1 is comparable with the chromophore module, termed CphΔ2 or Cph1N514, which ranges from M1 to E514 and which has been characterized in numerous studies (*6*, *10*, *30*, *38*). The F2 and F3 chromopeptides differ in their N-terminal cleavage site, which is located to next to T64 and L81, respectively, while the C-terminal cleavage site R472 is identical. The latter amino acid is located in the PHY domain and is conserved in all bacterial and plant phytochromes known to date. Both N-terminal cleavage sites are also located in the PAS domain.

Photoconversion during Trypsin Digestion. A 15 min digest produces samples in which either F1 or F2/F3 dominates. To obtain difference spectra of these samples for spectroscopic characterization of the fragments, we photoconverted digested samples with alternating red/far-red light (Figure 2). Since the protease was still active during irradiation and measuring, we analyzed aliquots after each measuring cycle by SDS−PAGE to check for possible proteolysis. The far-red-pretreated sample, which contains predominately F2 and F3 chromopeptides, gave a difference spectrum with a rather low Pfr absorption; the Pr to Pfr absorbance ratio was ca. 2.4, much higher than the corresponding value of undigested Cph1, which ranged between 0.9 and 0.95. The Pfr maximum of the degraded sample was blue shifted by 10 nm, and the Pr maximum was also slightly blue shifted (Figure 2, spectrum "B − C"). A second difference spectrum (Figure 2, spectrum "D − E") was comparable with the first one but showed a further reduction of the Pr absorption, which might result from ongoing degradation of the chromopeptides. When red-pretreated Cph1 was used for photoconversion experiments, complete digestion of F1 into F2/F3 during the 5 min of far-red irradiation was observed (Figure 2, compare G and H). Thus, the F2 and F3 cleavage sites of the F1 fragment become exposed upon photoconversion from Pfr to Pr. The first difference spectrum which was obtained with this sample (Figure 2, spectrum "H − G") is a difference spectrum between the Pr form of F2/F3 and the Pfr form of F1. The Pfr part was comparable with the full-length adduct, and the shape of the Pr part was similar to the F2/F3 fragments obtained by direct Pr digestion. After another round of photoconversion, during which only the F2/F3 fragments were present, the Pfr absorption was also reduced (Figure 2, spectrum "J − I"). Thus, the drastic loss of Pfr absorption and the blue shift of the absorption maximum by 10 nm are clearly correlated with the transition from F1 to F2/F3, i.e., with the loss of R472 to R520 in the C-terminus and R55 to R63 (or R80) in the N-terminus of F1.

In another experiment, we followed the light-induced degradation of F1 to F2/F3 kinetically (Figure 3). Red

Table 1: Summary of Trypsin and V8 Cleavage Sites of Cph1[a]

protease	fragment	apparent mass on SDS−PAGE (kDa)	preferentially after red (Pfr) or far-red (Pr) irradiation	N-terminal cleavage site	C-terminal cleavage site	calcd mass (kDa)
trypsin	F1	52	Pfr	R55/S56	R520/N521	53
	F2	49	Pr	R63/T64	R472/Q473	47
	F3	43	Pr	R80/L81	R472/Q473	45
endoproteinase Glu-C (V8)	F4	47	Pfr	E16/T17	N449/W450	49
	F5	35	Pfr	E16/T17	E335/A336	36
	F6	34	Pr	E16/T17	E323/T324	35
	F7	26	Pfr			
	F8	24	Pr	E120/L121	E323/T324	23

[a] The sequence of F7 is unknown, and the sequence of F8 is only tentative.

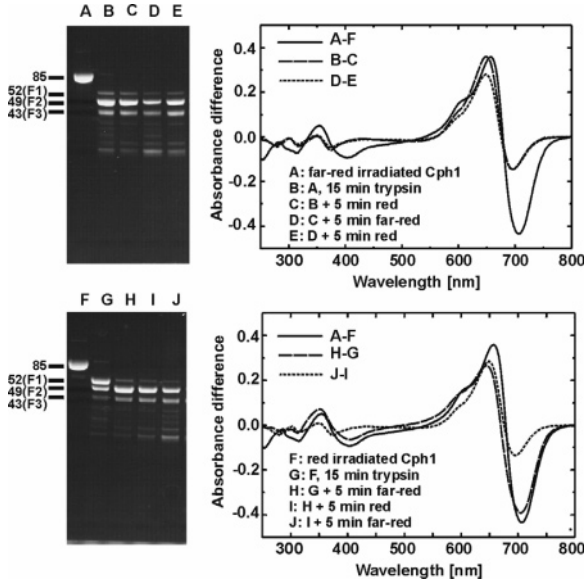

FIGURE 2: Photoconversion measurements during trypsin proteolysis. Above: far-red irradiated Cph1 (A) was incubated for 15 min with trypsin (B), and the sample was then irradiated consecutively with red (C), far-red (D), and red (E); the duration of each irradiation was 5 min. Below: red-irradiated Cph1 (F) was incubated for 15 min with trypsin (G) and then subsequently irradiated with far-red (H), red (I), and far-red (J). SDS−PAGE and detection by Zn^{2+}-induced fluorescence (left panels) show that chromopeptides of the far-red-treated sample remain quite stable during photoconversion, but the F1 chromopeptide of the red-pretreated sample degraded to F2 and F3 during the first far-red treatment. The difference spectra shown in the right panels are calculated from the absorbance measurements of samples A to J as indicated; A − F is the difference spectrum of undigested Cph1.

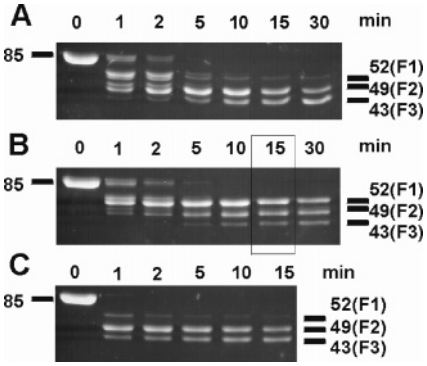

FIGURE 3: Trypsin digestion of Cph1, SDS−PAGE, and chromopeptide detection by Zn^{2+}-induced fluorescence. The incubation time is given above each panel. (A) Far-red irradiated Cph1 (Pr), (B) red-irradiated Cph1 (Pfr), and (C) the 15 min sample of (B) (delineated) irradiated with far-red to convert the chromopeptides into Pr. The apparent molecular size in kDa is indicated on the left and right side of each panel.

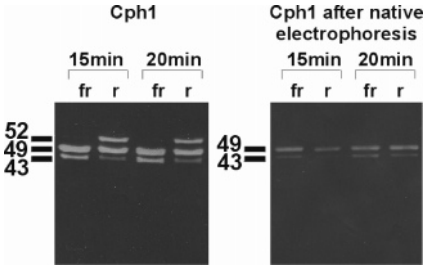

FIGURE 4: Trypsin digestion of normal Cph1 (purified affinity chromatography, left panel) and monomeric Cph1, which was obtained by an additional native electrophoresis step (right panel), Zn^{2+}-induced fluorescence. The apparent molecular size (kDa) of the chromopeptides is given on the left side of each panel.

irradiated Cph1 was first digested for 15 min and then converted by far-red to Pr; digestion was monitored by SDS−PAGE and Zn^{2+}-induced fluorescence at defined time intervals (Figure 3C). Within 1−2 min after the start of Pfr to Pr photoconversion, the degradation of the F1 fragment into F2/F3 was almost complete. It should be noted that photoconversion takes about 1 min under our irradiation conditions; thus the degradation time is probably shorter. In the control experiment, in which full-length Cph1 was digested in its Pr form, fragments with the size of F2 appeared after 2 min, but digestion into F2/F3 was completed only after ca. 10 min. Taken together, the F2/F3 cleavage sites are better accessible in the F1 fragment than in the full-length protein and, after F1 production, more exposed in the Pr than in the Pfr form. The accessibility can be based on monomer/dimer formation in both cases. Histidine kinases are sites of protein dimerization, and full-length Cph1 appears as a dimer (*24*, *30*). As discussed in ref *30*, the chromophore module of Cph1 (comparable with F1) might be monomeric in the Pr and dimeric in the Pfr form.

The effect of monomerization on trypsin digestion was tested with full-length Cph1 which was purified by native electrophoresis. Caused by transient alkaline pH, a subfraction of loaded Cph1 elutes from electrophoresis gels as monomeric protein, as judged by size exclusion chromatography (*24*). These samples are also characterized by their lack of autophosphorylation. Since histidine kinases always act as dimers, the lack of phosphorylation is another indication for the monomeric state. When electrophoretically purified Cph1 was treated with trypsin for 15 or 20 min, only the F2 and F3 fragments were formed, whereas the F1 fragment was missing. Furthermore, there was no difference between the red- and far-red-treated sample (Figure 4). Therefore, the F2/F3 cleavage sites become unprotected upon Cph1 monomerization.

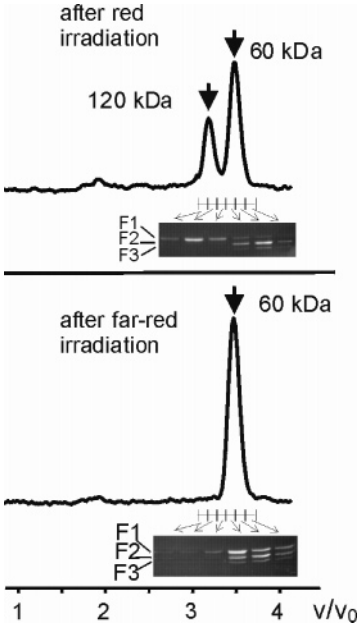

FIGURE 5: Size exclusion chromatography of F1, F2, and F3. Red irradiated Cph1 (10 μM) was digested for 15 min with trypsin, proteolysis was stopped by trypsin inhibitor, and the sample (200 μL) was subjected to size exclusion chromatography. The elution volume divided by the void volume (v_0) is given on the *x*-axis. Chromopeptide elution was monitored at 365 nm (*y*-axis, relative values), and the indicated fractions (500 μL each) were subjected to SDS−PAGE and Zn^{2+}-induced fluorescence. Above: the sample was kept in the red irradiated state (predominately Pfr). Below: before column separation, the sample was converted by far-red into the Pr form. The apparent molecular size at the position of the peaks (arrows) as estimated from calibration markers is indicated.

In another experiment, we tested by size exclusion chromatography whether F1 can switch between dimer and monomer upon Pfr−Pr photoconversion. To this end, we digested red irradiated Cph1 to obtain an F1/F2/F3 mixture, stopped the proteolysis reaction by trypsin inhibitor, and subjected the sample to size exclusion chromatography for molecular size determination. Eluted fractions were subjected to SDS−PAGE and Zn^{2+} fluorescence to distinguish between F1, F2, and F3. As shown in Figure 5 (upper panel), the F1 fragment eluted with an apparent molecular mass of 120 kDa, which is about twice the size of a single F1 molecule. F1 was clearly separated from the F2 and F3 fragments, which eluted with an apparent molecular mass of 60 kDa. UV−vis spectroscopy showed that F1 eluted as pure Pfr; the F2/F3 mix contained Pr and Pfr (data not shown). Please note that the sample was only irradiated before proteolysis and chromatography and that this irradiation produces about 70% Pfr. The distribution of fragments in the Pr and Pfr state is unequal after proteolysis and chromatography. The Pr absorbance maximum of F1 was at 648 nm and thus blue shifted as compared to full-length Cph1 (655 nm), whereas the position of the Pfr maximum was unchanged (702 nm; see also Figure 2). When the digested sample was irradiated with far-red before size exclusion chromatography to convert the chromopeptides into the Pr form, F1, F2, and F3 eluted together with an apparent molecular mass of 60 kDa. The size exclusion experiment shows that F1 is dimeric in its Pfr form and monomeric in its Pr form. The F2 and F3 fragments did not show this light-dependent behavior and appear always monomeric.

Proteolysis with Endoproteinase Glu-C (V8), SDS−PAGE, and UV−Vis Spectrometry. Cph1 was also subjected to endoproteinase Glu-C (V8) digestion (Figure 6A). After 1 min proteolysis, six chromopeptides of 85, 72, 61, 48, 35, and 26 kDa and two additional chromophore-free fragments of 40 and 31 kDa were obtained. During the initial 25 min of proteolysis, the peptide pattern was more or less unchanged and did not differ between both light pretreatments. A clear difference between Pr and Pfr was obtained when Cph1 was digested for 60 min or longer. In these samples, the 85 kDa chromopeptide (most likely the full-length protein) and the 72 and 61 kDa chromopeptides as well as the 40 and 31 kDa chromophore-free peptides were lost. The difference between both light pretreatments was most prominent after an incubation time of 24−48 h. The red-treated sample contained five chromopeptide fragments of 47, 35, 34, 26, and 24 kDa, which are denominated F4, F5, F6, F7, and F8, respectively. The far-red-treated sample contained only the F6 and F8 chromopeptides. Thus, the cleavage sites which form F6 and F8 are more protected in the Pfr than in the Pr form. The F6 and F8 fragments in the red-treated samples were probably obtained from the residual 30% Pr. For incubation times above 60 min, all chromophore-free fragments were smaller than 10 kDa. The band intensity of most of those bands was indistinguishable between both light treatments, but the intensity of a 3 kDa fragment was stronger in the red-treated sample. As in the case of trypsin digestion, absorbance maxima of Pr and Pfr shifted to lower wavelength upon V8 digestion (Figure 6B). However, the 48 digest was still photoactive (Figure 6C). The far-red-pretreated sample contains only the F6 and F8 chromopeptide fragments. Judging from the amplitude of the difference spectrum, both fragments were photoactive.

Mass Spectrometry of V8 Fragments. The sequences of F4, F5, and F6 were determined by mass spectrometry in the same way as described above for F1 to F3. The border subfragments of F4 to F6 were confirmed independently because the corresponding subfragments which have both a trypsin and a V8 cleavage site were detected in the mass spectrometer. The sequence of V8 chromopeptides is outlined in Figure 6D and summarized in Table 1. F4, F5, and F6 were produced by the same N-terminal cleavage site between E16 and T17. This site is located just outside the PAS domain. The C-terminal N449 of F4, located in the PHY domain, is an unusual cleavage site for V8, which is specific for Glu (=E). N449 must be rather exposed to the solvent to compensate for the reduced V8 activity. The C-terminal E335 of the F5 fragment is located between the GAF and the PHY domain, whereas the C-terminal E323 of the F6 fragment lies within the C-terminal edge of the GAF domain. To obtain sequence information of F7 and F8, both chromopeptides were digested with trypsin and analyzed by MALDI-TOF. In the case of F8, peptides from amino acids 155−310 were detected; in this case we could not detect the border subfragments. Assuming that both ends of F8 are formed by glutamate cleavage, two cleavage sites on each end are possible to yield fragments of the detected molecular size, namely, E120/L121, E122/P123 (in the N-terminus) and E323/T324, E333/H334 (in the C-terminus). We assume that F8 ranges from L121 to E323, which corresponds to a calculated molecular mass of 23660 Da. The C-terminal cleavage sites of F6 and F8 would then be identical. F7 was

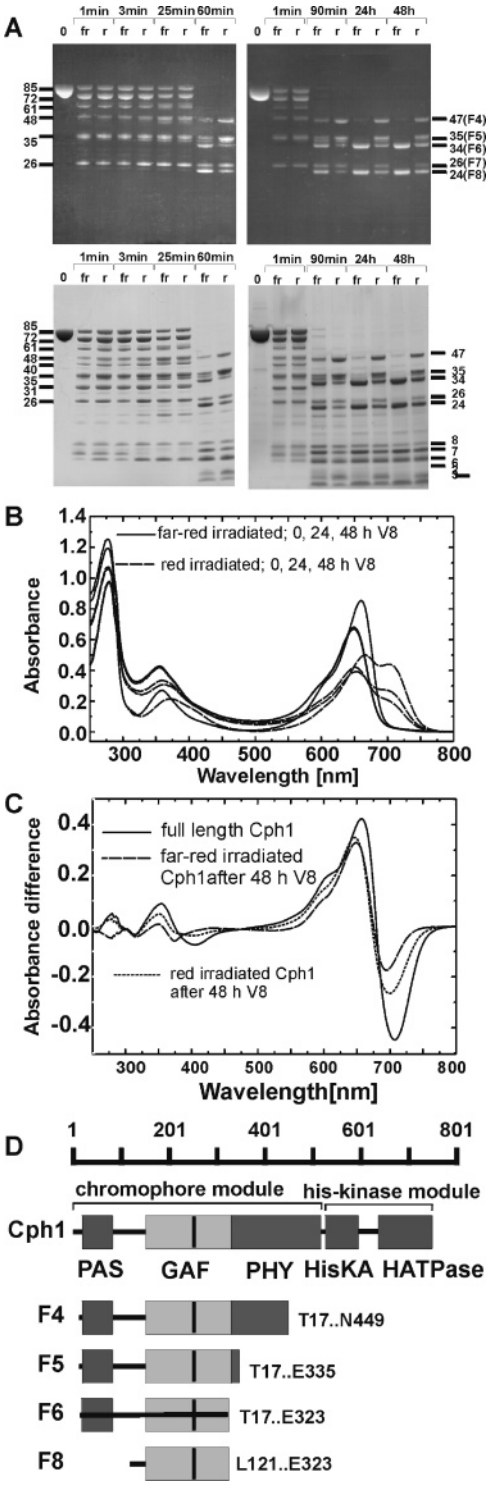

FIGURE 6: Endoproteinase Glu-C (V8) digestion. (A) SDS−PAGE. Cph1 was irradiated with saturating far-red (fr) or red (r) as indicated and incubated for 1 min to 48 h with V8 protease. 0 = undigested Cph1 control. Above: Zn^{2+}-induced fluorescence. Below: Coomassie stain. The apparent molecular size (kDa) of particular fragments is indicated on the left and right side of the panels. Chromopeptides of the 48 h digestions are denominated F4, F5, F6, F7, and F8. (B) UV−vis spectra of Cph1 during V8 proteolysis after far-red (straight lines) and red irradiation (dashed lines). The absorption in the red wavelength region decreases over time. (C) Difference spectra of red- and far-red irradiated Cph1 after 48 h V8 digestion in comparison with full-length Cph1; the spectra were measured as in Figure 2. (D) Domain structure of Cph1 and proteolytic fragments F4 to F6 and F8 (the sequence of F8 is tentative; see text and Table 1). The position of the chromophore-binding cysteine is indicated by a black line.

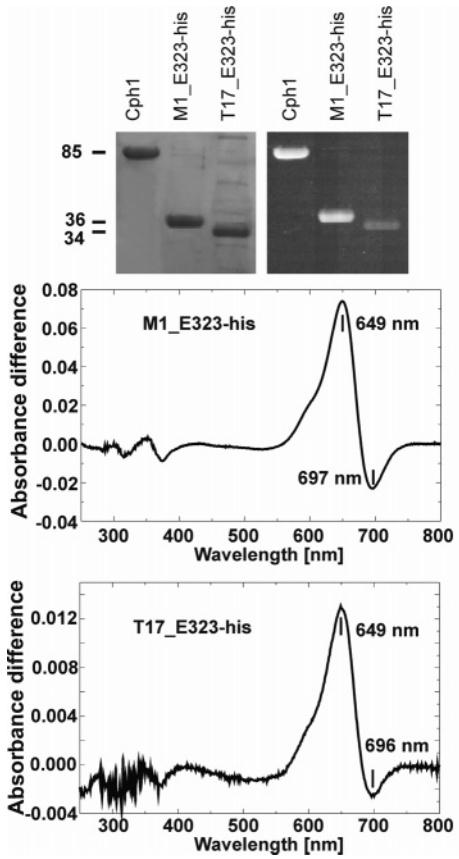

FIGURE 7: SDS−PAGE and photochemistry of recombinant Cph1 fragments. M1_E323-his and T17_E323-his were expressed in *E. coli*, purified by Ni affinity chromatography, and mixed with excess PCB. The upper panels show Coomassie stain (left) and Zn^{2+} fluorescence (right) of an SDS gel. Peptide size (kDa) is given on the left. Both panels below show difference spectra of assembled adducts. The protein concentration was ca. 10 μM.

eluted from SDS−PAGE as a mixture with a chromophore-free peptide, which was detected by MALDI-TOF. It was therefore not possible to obtain sequence information for F7.

Recombinant F6. The smallest photoactive fragments that arose from proteolysis experiments are F6, F7, and F8. We made an expression clone which encodes for a His-tagged F6 fragment, termed T17_E323-his. Another clone which encodes for the same peptide and the 16 amino acids of the Cph1 N-terminus was also made; this peptide is termed M1_E323-his. After expression and affinity purification, both peptides were tested for PCB assembly and photoconversion. Both peptides incorporated the PCB chromophore, as judged by Zn^{2+} fluorescence (Figure 7), but the amount of chromophore bound to T17_E323-his was rather low. In addition, both adducts showed red/far-red reversible absorbance changes between Pfr and Pr but had a rather low Pfr absorption. The Pr/Pfr absorbance ratio of difference spectra was 3.5 for M1_E323-his and 5.0 for T17_E323-his; the corresponding value was 0.9−0.95 for full-length Cph1. Qualitatively, the difference spectra resemble those of V8-digested Cph1-Pr, which contains F6 and F8 (Figure 6C), although in the latter case the relative Pfr absorbance was higher (Pr/Pfr absorbance ratio of 2.0). The recombinant fragments are thus differentially folded than the digestion products. A recombinant peptide which ranges from L121 to E323 and corresponds to the putative F8 fragment did not incorporate any chromophore (data not shown).

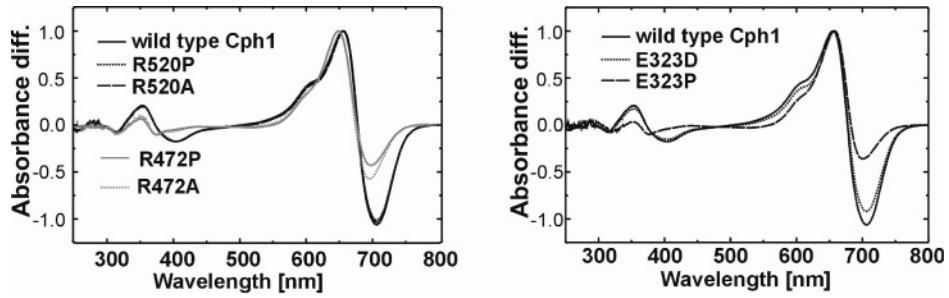

FIGURE 8: Difference spectra of wild-type Cph1 and mutants R520P, R520A, R472P, R472A (left panel), E323D, and E323P (right panel). Please note that the spectra of R520P and R520A are almost identical with that of the wild type.

Analysis of Site-Directed Mutants. Light-induced conformational changes of the N-terminal chromophore module must be transduced to the C-terminal histidine kinase to modulate autophosphorylation activity. We mutated three amino acids that were identified by our proteolysis experiments, R520, R472, and E323, to study the impact on intramolecular signal transduction. For each position, two replacements were performed. Arginine was replaced by either proline or alanine, and glutamate was replaced by either proline or aspartate. Thus, six different mutants, R520A, R520P, R472A, R472P, E323D, and E323P, were obtained. Adducts of the R520A and R520P mutants were spectrally almost indistinguishable from adducts of wild-type Cph1 (Figure 8). This is reasonable, because the mutation lies outside the chromophore module (amino acids 1−514), which is spectrally identical with the full-length protein (*6*, *10*, *30*). The adducts of R472P and R472A had blue-shifted Pr and Pfr absorption maxima (from 659 to 650 nm and from 708 to 699 nm, respectively) and a reduced relative Pfr absorption. These mutants are thus spectrally similar to F2 or F3. In E323P and E323D adducts, the positions of the Pr absorption maxima were unchanged, but both adducts had a reduced relative Pfr absorption. This reduction was more prominent in the E323P adduct, which also had a blue-shifted Pfr absorption maximum (from 708 to 702 nm). To test for alterations of quaternary structure, we subjected the mutants to size exclusion chromatography. Wild-type Cph1 elutes with the dominant peak at the position of the dimer (ref *24* and Figure 9). The elution profiles of E323P and E323D were comparable with the wild-type protein, although both constructs had a slightly bigger apparent molecular weight, which might be indicative for a different shape of the molecule (Figure 9). Dimer peaks were also present in all other constructs. R472A and R520A had an additional monomer peak around 100 kDa. This finding is interesting, because dimerization of full-length Cph1 is thought to be mediated by the histidine kinase module. The mutants R520A, R520P, and R472A also showed increased aggregate formation.

Histidine kinase activity of Cph1 is light regulated; its activity is strong in the Pr and weak in the Pfr form, with a ratio of about 4.5 between far-red- and red-treated samples (ref *10* and Figure 10C). To test for the impact of the mutations on the modulation of histidine kinase activity, all mutants were subjected to autophosphorylation assays after saturating red or far-red irradiation. A typical autoradiogram is shown in Figure 10A, and quantifications of three independent experiments are presented in Figure 10B,C. The phosphorylation pattern was different in each mutant, and all mutants differed from the wild type in this respect. In

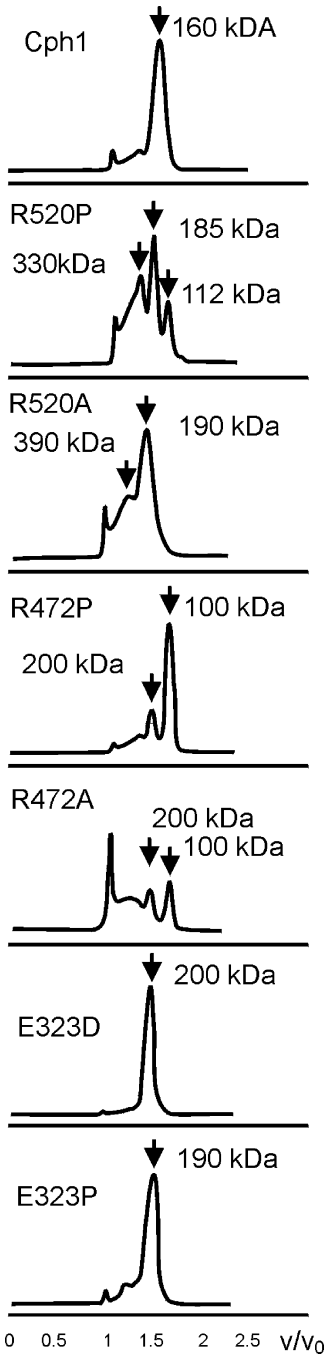

FIGURE 9: Size exclusion profiles of Cph1 and mutant adducts. Samples (protein concentration 10 μM) were converted into the Pr form and subjected to size exclusion chromatography. The elution volume divided by the void volume (v_0) is given on the *x*-axis. Elution was monitored at 280 nm (*y*-axes; relative absorbance).

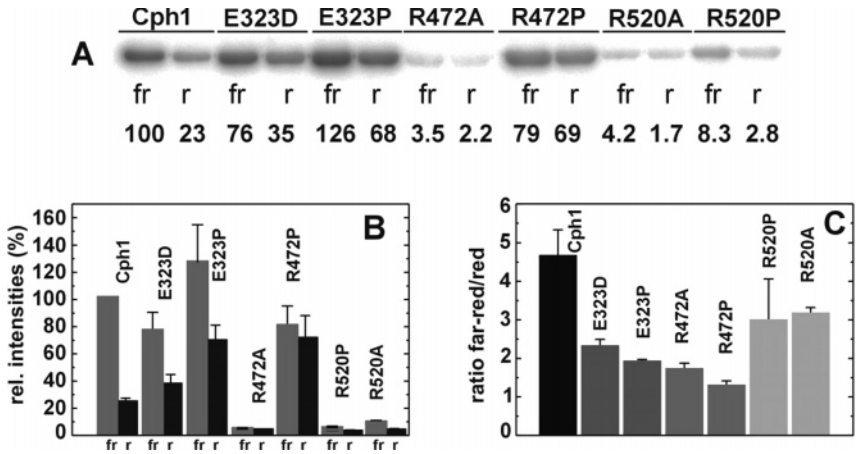

FIGURE 10: Autophosphorylation of wild-type and mutant Cph1. Cph1 samples were irradiated with either far-red (fr) or red (r), incubated with [γ-^{32}P]ATP in darkness, separated on SDS−PAGE, and blotted to PVFD membrane. (A) Example for an autoradiogram of the Cph1 band. The protein load was identical in each lane. Relative phosphorylation intensities are given below (Pr of wild type = 100). (B) Phosphorylation intensities of three different experiments as in (A) (mean values ± SE). (C) Phosphorylation ratio between the far-red- and the red-treated samples (mean values ± SE).

R472A, R520A, and R520P, the phosphorylation was drastically reduced. This finding correlates with the tendency to form protein aggregates. In E323D, E323P, and R472P, the phosphorylation of the far-red irradiated sample (Pr) was comparable with the wild type, but the phosphorylation of the red-irradiated samples was stronger than that of the wild-type control. In all six mutants, the phosphorylation ratio between the far-red and the red irradiated sample was significantly lower than in the wild type (Figure 10C).

DISCUSSION

Limited proteolysis has been performed with different plant phytochromes to probe for conformational changes upon Pr to Pfr conversion. Bacterial phytochromes differ from plant homologues in several aspects: they are smaller and they act as light-regulated histidine kinases. In the present work, differentially irradiated Cph1 adducts were subjected to limited proteolysis. These studies help to understand the role of different regions of the protein with respect to spectral integrity and give an insight into intramolecular signal transduction from the chromophore module to the histidine kinase.

Spectral Integrity. Proteolysis alters spectral properties of Cph1 in several ways. Absorbance maxima of Pr and Pfr shift to shorter wavelengths, and absorbance of both forms becomes reduced. All chromopeptides that arise from trypsin or V8 digestion are photoactive. Both the PHY domain, which is lacking in F5 to F8, and the N-terminal PAS domain, which is lacking in F3 and F8, are dispensable for photoactivity. Small photoactive fragments of plant phytochrome with molecular sizes of 16 kDa (*12*) and 39 kDa (*9*, *11*) have been described. The N-terminal 22 kDa GAF subdomain of Cph2, the second phytochrome of *Synechocystis*, which differs from typical phytochromes by its unique domain structure, incorporates chromophore and reveals weak photoactivity (*8*). Our finding that the 24 kDa F8 chromopeptide fragment of Cph1 is photoactive matches with these observations. It has recently been shown that the chromophore binding site of biliverdin-binding phytochromes lies in the N-terminus of the protein, close to the PAS domain (*7*, *23*). Although this part of phytochrome therefore forms a part of the chromophore pocket, it is obviously not required for photoactivity. In the present study we have found that an expressed peptide, T17_E323 (equivalent to F6), which lacks the N-terminal 16 amino acids of Cph1 shows reduced chromophore incorporation as compared to the M1_E323 peptide. The 16 N-terminal amino acids play thus an important role in the lyase reaction of recombinant Cph1 fragments, for example, by stabilizing the protein conformation.

The PHY domain shifts Pr and Pfr absorbance toward longer wavelengths, as seen from the difference spectra of F2 to F8, in which the PHY domain is partially or completely lacking. The PHY domain seems also to be important for the rather high extinction coefficient of Pr and Pfr. Its impact on the Pfr spectrum is stronger than on Pr, because in F2 to F8 the Pfr form differed more from the full-length protein than the Pr form. In the mutant E323P, the PHY domain appears uncoupled from the rest of the chromophore module. This mutant has a rather low Pfr absorbance but a normal Pr spectrum. Spectra of the R472A and R472P mutants, in which the PHY domain is probably disturbed, also confirmed the proposed spectral function of the PHY domain. Truncated plant phytochromes, either recombinant or proteolysis products, in which the PHY domain is at least partially lacking are also characterized by their reduced relative Pfr absorbance and blue shift of the Pfr absorbance maximum (*9*, *11*, *39*). On the basis of sequence similarity among phytochromes we predict that the PHY domain has a more or less universal spectral function in all phytochromes.

Pr and Pfr Specific Exposure of Cleavage Sites. The histidine kinase subunit must be rapidly degraded into small fragments, because a chromophore-free peptide of the corresponding molecular mass (N521 to N748 with the additional histidine tag RSHHHHHH has a size of 28 kDa) was not obtained. In the early stages of trypsin and V8 digestions, a 31 kDa and other large chromophore-free fragments were formed, but the band intensities were rather weak and the fragments disappeared earlier than the chromopeptide fragments. In general, chromophore-free peptides were much less stable than chromopeptides. Thus, the histidine kinase subunit is more sensitive to protease attack

or less compact than the chromophore module. From our proteolysis experiments, we obtained no information on conformation-specific exposure of a cleavage site in the histidine kinase module. Of all identified cleavage sites, R520 and R472 are the most interesting ones. R520 lies in the hinge region between the chromophore module and histidine kinase. In plant phytochromes, the hinge region is also sensitive to protease attack (*16*), but there was no conformation-specific effect. Because, in Cph1, R520 is cleaved slightly faster in the Pfr than in the Pr form, this implies that in this phytochrome the hinge region undergoes subtle changes during photoconversion. The time course of trypsin digestion suggests also that F1 is more stable in the Pfr form because formation of F2/F3 is inhibited in Pfr (Figure 3B,C). The cleavage sites at R472, R63, and R80 are thus protected in the Pfr form. When proteolysis experiments were performed with the Cph1 monomer, which was isolated by native electrophoresis, the protein was directly degraded to F2/F3, irrespective of the conformation of Cph1. This reminds us of the results of Park et al. (*31*), who found no differential cleavage pattern with their Cph1 expression clone, which probably produces monomeric Cph1. Since F1 was only stable in the dimer, we assume that dimer formation protects the R472 cleavage site. In the full-length protein, Cph1 dimers are formed by the histidine kinase. It has been shown by fluorescence resonance energy transfer that the deletion construct Cph1Δ2 (amino acids 1−514), which consists of the chromophore module without histidine kinase, can also form dimers, but subunit interaction is much weaker than in full-length Cph1 (*38*). In the present paper we analyzed light-dependent dimerization of F1 by size exclusion chromatography (Figure 5). F1 appears as a dimer in the Pfr and as a monomer in the Pr form. Since fragments F2 and F3 did not show this light-dependent effect (Figure 5), the dimerization domain of F1 is either located between amino acids 472 and 520 or between amino acids 56 and 64 (for comparison of F1 and F2, see Figure 1C) or in both regions. Further experiments with recombinant proteins are required to differentiate between these possibilities. Taken together, formation of F2/F3 by trypsin seems only possible in the monomeric form. In full-length Cph1, dimerization is mediated by the histidine kinase; therefore, F2 and F3 are only formed after removal of the C-terminus. If the F1 fragment is in the Pfr form, R472 is protected (therefore, F1 accumulates), but in the Pr form, F1 monomerizes and proteolysis into F2/F3 proceeds rather rapidly (see cartoon in Figure 11). Protein alignments showed that R472 is conserved in all plant and bacterial phytochromes and lies within a conserved peptide motive P**R**X_1SFX_2X_3W/F, which is the region of the highest homology outside the GAF domain. (X_1 stands for T, I, H, K, Q, R, S, L, or G; X_2 is either E, D, A, K, Q, or T; X_3 is either I, R, T, L, A, or Q; the last amino acid is an F in plants and a W in bacteria.) This homologous region could be important for light-dependent subunit interaction in all phytochromes. The F2 and F3 fragments are missing the region C-terminal of R472, which correlates with their inability to form dimers. Quite interestingly, dark reversion of one subunit of dimeric plant phytochromes is affected by the conformation of the other subunit (*40*). Judging from recent results on the function of the PHY domain with respect to dark reversion (*39*), subunit communication of plant phytochromes seems to be mediated

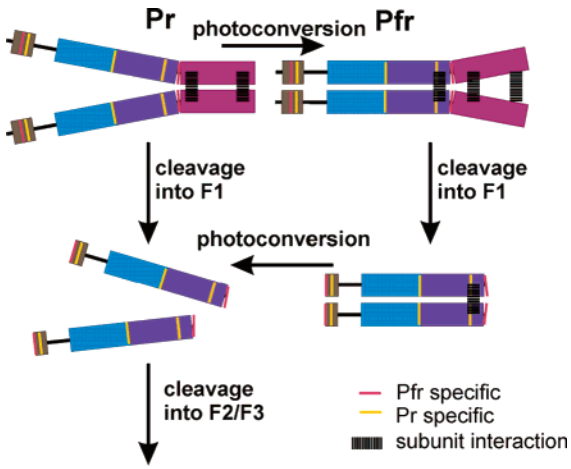

FIGURE 11: Model on photoconversion of Cph1 and generation of trypsin fragments F1, F2, and F3. The following colors are used for protein domains: PAS domain, gray; GAF domain, light blue; PHY domain, dark blue; histidine kinase module, violet. PAS, GAF, and PHY domains constitute the chromophore module. Yellow and red lines indicate the position of Pr and Pfr specific cleavage sites, respectively. In the full-length protein, chromophore domain subunits come closer together upon Pr to Pfr conversion. As a result, the histidine kinase subunits are dispersed, resulting in a reduced autophosphorylation activity. Trypsin treatment releases the F1 fragment, which rapidly degrades into F2/F3 if Cph1 is in the Pr form. In the Pfr form, F1 accumulates because the F2/F3 cleavage sites are protected by subunit interaction. The positions of protease cleavage sites are indicated by red (Pfr specific) and yellow (Pr specific) lines.

by the PHY domain. The A587T mutant of *Arabidopsis* phytochrome B, which results in a reduction of physiological activity and nuclear mislocation (*41*), is also characterized by increased dark reversion (*39*). Alanine 587 of phytochrome B is located at the X_2 position of the above alignment. In the G564E and G564A mutants of the same phytochrome, dark reversion is also affected (*39*, *42*). Glycine 564 of phytochrome B could also be important for subunit interaction within the dimer, although the corresponding amino acid of Cph1, G451, lies within the F2 and F3 fragments that do not seem to dimerize. Cph1 does not undergo dark reversion, but our results on subunit interaction might give a clue for the understanding of plant phytochrome dark reversion.

Intramolecular Signal Transduction. Dimer formation is important for the function of histidine kinases, because the histidine substrate of one subunit is phosphorylated by the kinase domain of the other subunit (*43*). The kinase activity might be regulated by modulating the distance between both subunits. In Cph1, phosphorylation is stronger in the Pr than in the Pfr form. Possibly, the increased subunit interaction of the chromophore module upon Pfr photoconversion causes an increase in the distance between both histidine kinase subunits, thereby reducing enzymatic activity, as outlined in the model of Figure 11. In the present study, six different point mutants were analyzed for light-regulated autophosphorylation. Although a point mutation can affect the general folding of a protein subdomain, as shown by size exclusion chromatography (Figure 9), and mutant effects may thus not be directly related to a single amino acid, the phosphorylation results allowed to gain a deeper insight into intramolecular signal transduction of Cph1. The hinge region mutants R520A and R520P show that this region plays an important

role in histidine kinase phosphorylation: in both mutants phosphorylation is very weak. In size exclusion studies (Figure 9) these mutants tended to form aggregates and monomers. It could be that the hinge region of the mutants is misfolded in such a way that the histidine kinase subunits are drawn apart from each other and that this event results in monomer formation and aggregation. The third mutant with a low phosphorylation activity is R472A; this mutant also formed monomers and aggregates (Figure 9) and appears thus similar to the hinge region mutants. However, R472 is part of the chromophore module. The mutation could have an indirect effect on the activity of the histidine kinase, e.g., by reducing the possibility to form dimers and by inducing Cph1 aggregation. In all other mutants, namely, E323D, E323P, and R472P, aggregate formation is not increased. Therefore, mutagenesis induced probably more subtle changes of protein structure. Quite interestingly, these mutants displayed high levels of Pr *and* Pfr autophosphorylation, and the Pr/Pfr phosphorylation ratio was smaller than that of wild-type Cph1. From these mutant data the impression arises that, in wild-type Cph1, histidine phosphorylation is actively inhibited upon Pr to Pfr photoconversion. This is consistent with the scissors model discussed above and outlined in Figure 11, in which chromophore module subunits move (actively) closer together and histidine kinase subunits are torn apart upon photoconversion.

ACKNOWLEDGMENT

We thank Norbert Michael, Sabine Buchert, Connie Görick, and Sabine Artelt for technical help.

REFERENCES

1. Montgomery, B. L., and Lagarias, J. C. (2002) Phytochrome ancestry: sensors of bilins and light, *Trends Plant Sci. 7*, 357−366.
2. Lamparter, T., and Hughes, J. (2003) Phytochromes and phytochrome-like proteins in cyanobacteria, in *Photoreceptors and light signalling* (Batschauer, A., Ed.) pp 203−227, Royal Society of Chemistry, Cambridge, U.K.
3. Rüdiger, W., Thümmler, F., Cmiel, E., and Schneider, S. (1983) Chromophore structure of the physiologically active form (Pfr) of phytochrome, *Proc. Natl. Acad. Sci. U.S.A. 80*, 6244−6248.
4. Andel, F., Hasson, K. C., Gai, F., Anfinrud, P. A., and Mathies, R. A. (1997) Femtosecond time-resolved spectroscopy of the primary photochemistry of phytochrome, *Biospectroscopy 3*, 421−433.
5. Heyne, K., Herbst, J., Stehlik, D., Esteban, B., Lamparter, T., Hughes, J., and Diller, R. (2002) Ultrafast dynamics of phytochrome from the cyanobacterium *Synechocystis*, reconstituted with phycocyanobilin and phycoerythrobilin, *Biophys. J. 82*, 1004−1016.
6. van Thor, J. J., Borucki, B., Crielaard, W., Otto, H., Lamparter, T., Hughes, J., Hellingwerf, K. J., and Heyn, M. P. (2001) Light-induced proton release and proton uptake reactions in the cyanobacterial phytochrome Cph1, *Biochemistry 40*, 11460−11471.
7. Lamparter, T., Carrascal, M., Michael, N., Martinez, E., Rottwinkel, G., and Abian, J. (2004) The biliverdin chromophore binds covalently to a conserved cysteine residue in the N-terminus of Agrobacterium phytochrome Agp1, *Biochemistry 43*, 3659−3669.
8. Wu, S. H., and Lagarias, J. C. (2000) Defining the bilin lyase domain: lessons from the extended phytochrome superfamily, *Biochemistry 39*, 13487−13495.
9. Gärtner, W., Hill, C., Worm, K., Braslavsky, S. E., and Schaffner, K. (1996) Influence of expression system on chromophore binding and preservation of spectral properties in recombinant phytochrome A, *Eur. J. Biochem. 236*, 978−983.
10. Yeh, K. C., Wu, S. H., Murphy, J. T., and Lagarias, J. C. (1997) A cyanobacterial phytochrome two-component light sensory system, *Science 277*, 1505−1508.
11. Reiff, U., Eilfeld, P., and Rüdiger, W. (1985) A photoreversible 39-kdalton fragment from the Pfr form of 124-kdalton oat phytochrome, *Z. Naturforsch., C: J. Biosci. 40*, 693−698.
12. Jones, A. M., and Quail, P. H. (1989) Phytochrome structure: Peptide fragments from a amino-terminal domain involved in protein-chromophore interactions, *Planta 178*, 147−156.
13. Lagarias, J. C., and Mercurio, F. M. (1985) Structure function studies on phytochrome. Identification of light-induced conformational changes in 124-kDa Avena phytochrome in vitro, *J. Biol. Chem. 260*, 2415−2423.
14. Jones, A. M., Vierstra, R. D., Daniels, S. M., and Quail, P. (1985) The role of separate molecular domains in the structure of phytochrome from etiolated *Avena sativa* l, *Planta 164*, 501−506.
15. Jones, A. M., and Quail, P. H. (1986) Quaternary structure of 124-kilodalton phytochrome from *Avena sativa* L, *Biochemistry 25*, 2987−2995.
16. Grimm, R., Eckerskorn, C., Lottspeich, F., Zenger, C., and Rüdiger, W. (1988) Sequence analysis of proteolytic fragments of 124-kilodalton phytochrome from etiolated *Avena sativa* L.: Conclusions on the conformation of the native protein, *Planta 174*, 396−401.
17. Schendel, R., Tong, Z., and Rüdiger, W. (1989) Partial proteolysis of rice phytochrome: comparison with oat phytochrome, *Z. Naturforsch., C 44*, 757−764.
18. Nakazawa, M., Hayashi, H., Yoshida, Y., and Manabe, K. (1993) Identification of surface-exposed parts of red-light- and far-red-light-absorbing forms of native pea phytochrome by limited proteolysis, *Plant Cell Physiol. 34*, 83−91.
19. Nakazawa, M., and Manabe, K. (1993) Differential exposure of tryptophan residues in the red and far-red light absorbing forms of phytochrome, as revealed by chemical modification, *Plant Cell Physiol. 34*, 1097−1105.
20. Lapko, V. N., Jiang, X. Y., Smith, D. L., and Song, P. S. (1998) Surface topography of phytochrome a deduced from specific chemical modification with iodoacetamide, *Biochemistry 37*, 12526−12535.
21. Yeh, K. C., and Lagarias, J. C. (1998) Eukaryotic phytochromes: Light-regulated serine/threonine protein kinases with histidine kinase ancestry, *Proc. Natl. Acad. Sci. U.S.A. 95*, 13976−13981.
22. Hübschmann, T., Jorissen, H. J. M. M., Börner, T., Gärtner, W., and Tandeau de Marsac, N. (2001) Phosphorylation of proteins in the light-dependent signaling pathway of a filamentous cyanobacterium, *Eur. J. Biochem. 268*, 3383−3389.
23. Lamparter, T., Michael, N., Mittmann, F., and Esteban, B. (2002) Phytochrome from *Agrobacterium tumefaciens* has unusual spectral properties and reveals an N-terminal chromophore attachment site, *Proc. Natl. Acad. Sci. U.S.A. 99*, 11628−11633.
24. Lamparter, T., Esteban, B., and Hughes, J. (2001) Phytochrome Cph1 from the cyanobacterium *Synechocystis* PCC6803: purification, assembly, and quaternary structure, *Eur. J. Biochem. 268*, 4720−4730.
25. Bhoo, S. H., Davis, S. J., Walker, J., Karniol, B., and Vierstra, R. D. (2001) Bacteriophytochromes are photochromic histidine kinases using a biliverdin chromophore, *Nature 414*, 776−779.
26. Hübschmann, T., Börner, T., Hartmann, E., and Lamparter, T. (2001) Characterisation of the Cph1 holo-phytochrome from *Synechocystis* sp. PCC 6803, *Eur. J. Biochem. 268*, 2055−2063.
27. Hughes, J., Lamparter, T., Mittmann, F., Hartmann, E., Gärtner, W., Wilde, A., and Börner, T. (1997) A prokaryotic phytochrome, *Nature 386*, 663.
28. Lamparter, T., Mittmann, F., Gärtner, W., Börner, T., Hartmann, E., and Hughes, J. (1997) Characterization of recombinant phytochrome from the cyanobacterium *Synechocystis*, *Proc. Natl. Acad. Sci. U.S.A. 94*, 11792−11797.
29. Borucki, B., Otto, H., Rottwinkel, G., Hughes, J., Heyn, M. P., and Lamparter, T. (2003) Mechanism of Cph1 phytochrome assembly from stopped-flow kinetics and circular dichroism, *Biochemistry 42*, 13684−13697.
30. Otto, H., Lamparter, T., Borucki, B., Hughes, J., and Heyn, M. P. (2003) Dimerization and inter-chromophore distance of Cph1 phytochrome from Synechocystis, as monitored by fluorescence homo and hetero energy transfer, *Biochemistry 42*, 5885−5895.
31. Park, C. M., Shim, J. Y., Yang, S. S., Kang, J. G., Kim, J. I., Luka, Z., and Song, P. S. (2000) Chromophore-apoprotein

interactions in *Synechocystis* sp. PCC6803 phytochrome Cph1, *Biochemistry 39*, 6349−6356.
32. Remberg, A., Lindner, I., Lamparter, T., Hughes, J., Kneip, K., Hildebrandt, P., Braslavsky, S. E., Gärtner, W., and Schaffner, K. (1997) Raman spectroscopic and light-induced-kinetic characterization of a recombinant phytochrome of the cyanobacterium *Synechocystis*, *Biochemistry 36*, 13389−13395.
33. Foerstendorf, H., Lamparter, T., Hughes, J., Gärtner, W., and Siebert, F. (2000) The photoreactions of recombinant phytochrome from the cyanobacterium *Synechocystis*: A low-temperature UV-Vis and FT-IR spectroscopic study, *Photochem. Photobiol. 2000*, 655−661.
34. Laemmli, U. K. (1970) Cleavage of structural proteins during the assembly of the head of bacteriophage T4, *Nature 227*, 680−685.
35. Berkelman, T. R., and Lagarias, J. C. (1986) Visualization of bilin-linked peptides and proteins in polyacrylamide gels, *Anal. Biochem. 156*, 194−201.
36. Carrascal, M., Carujo, S., Bachs, O., and Abian, J. (2002) Identification of p21Cip1 binding proteins by gel electrophoresis and capillary liquid chromatography microelectrospray tandem mass spectrometry, *Proteomics 2*, 455−468.
37. Sineshchekov, V., Hughes, J., Hartmann, E., and Lamparter, T. (1998) Fluorescence and photochemistry of recombinant phytochrome from the cyanobacterium Synechocystis, *Photochem. Photobiol. 67*, 263−267.
38. Borucki, B., Otto, H., Rottwinkel, G., Hughes, J., Heyn, M. P., and Lamparter, T. (2003) Mechanism of Cph1 phytochrome assembly from stopped-flow kinetics and circular dichroism, *Biochemistry 42*, 13684−13697.
39. Oka, Y., Matsushita, T., Mochizuki, N., Suzuki, T., Tokutomi, S., and Nagatani, A. (2004) Functional analysis of a 450-amino Acid N-terminal fragment of phytochrome B in Arabidopsis, *Plant Cell 16*, 2104−2116.
40. Hennig, L., and Schäfer, E. (2001) Both subunits of the dimeric plant photoreceptor phytochrome require chromophore for stability of the far-red light-absorbing form, *J. Biol. Chem. 276*, 7913−7918.
41. Chen, M., Schwab, R., and Chory, J. (2003) Characterization of the requirements for localization of phytochrome B to nuclear bodies, *Proc. Natl. Acad. Sci. U.S.A. 100*, 14493−14498.
42. Kretsch, T., Poppe, C., and Schäfer, E. (2000) A new type of mutation in the plant photoreceptor phytochrome B causes loss of photoreversibility and an extremely enhanced light sensitivity, *Plant J 22*, 177−186.
43. Stock, A. M., Robinson, V. L., and Goudreau, P. N. (2000) Two-component signal transduction, *Annu. Rev. Biochem. 69*, 183-215.

BI0484365